

Solution Combustion Synthesis and Structural Properties of YSrAl₃O₇: Tb Nanoparticles

Sheetal, S.P. Khatkar*, Rajni Arora, V.B. Taxak, Mandeep

*Maharshi Dayanand University, Rohtak-124001, India.
E-mail: *s_khatkar@rediffmail.com*

Abstract

Tb³⁺ doped YSrAl₃O₇ nanoparticles have been prepared by solution combustion synthesis process using urea as a fuel. Morphology and luminescent properties of Y_{1-x}SrAl₃O₇:xTb³⁺ (Tb = 5, 10 12 mol %) nanoparticles were characterized by scanning electron microscopy, transmission electron microscopy, fluorescence spectrometry and X-ray diffraction studies. The incorporation of Tb³⁺ activator in these nanoparticles has been checked by luminescence characteristics. The prepared nanoparticles under UV source revealed green luminescence. The emission spectra indicated the excellent green photoluminescent properties of YSrAl₃O₇:Tb³⁺ nanoparticles due to characteristics transition of Tb³⁺ ions from ⁵D₄ → ⁷F₅ at 544 nm (λ_{ex}=251 nm). The dependence of the luminescence intensity on Tb³⁺ ions concentrations and effect of heat treatment have also been discussed. The excitation spectrum of YSrAl₃O₇:Tb³⁺ was observed with maximum peak at 251 nm (λ_{em}=544 nm). From TEM studies it was observed that nanoparticles have average size from 10 nm to 22 nm. These nanoparticles may be used in the fields of high-performance luminescent devices, catalysts and other functional materials due to their exceptional electronic, optical and chemical characteristics arising from 4f electrons.

Keywords: YSrAl₃O₇:Tb³⁺, Nanoparticles, Urea, Green luminescence.

*Corresponding Author: Tel: +91 9813805666.

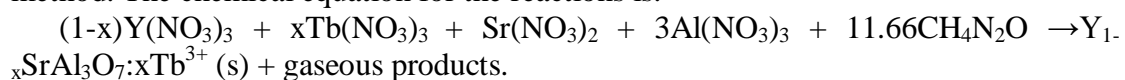
1. Introduction

Significant efforts have been devoted to synthesize and investigate an important family of inorganic materials having general chemical formula ABC_3O_7 (A=Ca, Sr, Ba; B= Y, La, Gd; C = Al, Ga) as these materials find various kinds of application in all-solid-state lasers, plasma display panels (PDP) for high definition TV (HDTV), mercury-free high intensity discharge lamps (HID), diode laser pumping and tunable laser generation [1-3]. The compounds have melitite structure [4-6]. The crystal structure is built up from CO_4 tetrahedra to form a tetragonal sheet-like arrangement. The sheet structure consists of five membered rings of CO_4 tetrahedra perpendicular to the c-axis and between the layers, A^{2+} and B^{3+} ions are distributed randomly in eight coordinated sites with Cs symmetry [7,8]. Rare-earth ions doped luminescent nanomaterials have attracted much attention of scientists recently, especially Eu^{3+} and Tb^{3+} , because of 4f electrons intra-configurational transitions, as the electrons are well shielded from neighboring ions so discrete and sharp energy levels are obtained in their compounds [9-12]. Solid state method requires high temperature and long calcination time for the preparation of phosphor materials. Even at high temperature ($\sim 1400^\circ\text{C}$) pure phase is not obtained and the particles are agglomerated. A large number of melitite structure compounds have been synthesized by solid state [4-6]. In addition, some other methods such as czochralski [13,14] and sol-gel [15-17] have been also used to synthesize phosphors. A non-toxic, low-cost, one-step and fast route combustion method has been employed to synthesize $GdCaAl_3O_7:Eu^{3+}$ [2], $LaCaAl_3O_7$ doped with variety of ns^2 and rare earth activators [7], Er^{3+}/Yb^{3+} co-doped $CaYAl_3O_7$ [18] and $CaYAl_3O_7:Eu^{3+}$ [19] phosphors. We have recently employed this combustion method to synthesize melitite structure $YCaAl_3O_7:Eu^{3+}$ nanoparticles and studied their photoluminescence characteristics [20]. In the present work, our aim is to prepare another important member of melitite structure family $YSrAl_3O_7:Tb^{3+}$ by fast route solution combustion method and compare high photoluminescence intensity of nanosized particles doped with different concentrations and calcined at different temperatures.

2. Experimental

2.1. Powder Synthesis

The starting reagents were high purity $Y(NO_3)_3$, $Al(NO_3)_3 \cdot 9H_2O$, $Sr(NO_3)_2$, $Tb(NO_3)_2 \cdot 6H_2O$ and urea. $Y_{1-x}SrAl_3O_7:xTb^{3+}$ was synthesized by solution combustion method. The chemical equation for the reactions is:



According to nominal composition of $Y_{1-x}SrAl_3O_7:xTb^{3+}$ ($x = 0.05, 0.10$ and 0.12), a stoichiometric amount of metal nitrates were dissolved in minimum quantity of deionized water in 200 mL capacity pyrex beaker. Then urea was added in this solution with molar ratio of urea to nitrates based on total oxidizing and reducing valencies of oxidizer and fuel (urea) according to concept used in propellant chemistry [21]. Finally

the beaker containing the solution was placed into a preheated furnace at 500°C . The material undergoes rapid dehydration and foaming followed by decomposition, generating combustible gases. These volatile combustible gases ignite and burn with a flame yielding voluminous solid. Urea was oxidized by nitrate ions and served as a fuel for propellant reaction. The powders obtained were again fired at 700°C to 1100°C for 3 h to increase the brightness.

2.2. Powder Characterization Techniques

The crystal phase of $\text{YSrAl}_3\text{O}_7:\text{Tb}^{3+}$ powders were characterized by Rigaku Ultima-IV X-ray powder diffraction with $\text{CuK}\alpha$ radiation to record the patterns in the 2θ range of $10\text{--}80^\circ$. The morphology and particle size were evaluated using Jeol JSM-6510 scanning electron microscope (SEM) and FEI-Morgagni-268D transmission electron microscope (TEM). The Fourier transform infrared (FT-IR) spectra were recorded using a Perkin Elmer spectrometer in the spectral range of $4000\text{--}400\text{ cm}^{-1}$ following KBr pellet technique. The excitation and emission spectra of the powders in the ultraviolet-visible region were evaluated at room temperature using a Hitachi F-7000 fluorescence spectrophotometer with Xe- lamp as the excitation source.

3. Results and Discussion

3.1. X-ray diffraction studies

The XRD patterns of $\text{Y}_{0.9}\text{Tb}_{0.1}\text{SrAl}_3\text{O}_7$ powders, as-prepared and calcined at different temperatures for 3h, are shown in fig.1. In strontium-ytterium aluminate YSrAl_3O_7 , the frames of the compounds are formed by five membered rings constructed from AlO_4^{5-} tetrahedral and between the layers Sr^{2+} and Y^{3+} ions are distributed randomly in eight coordinated sites with Cs symmetry [15]. XRD patterns of the as-prepared samples show many additional peaks corresponding to those of unreacted $\text{Sr}(\text{NO}_3)_2$ phase (JCPDS card no. 04-0310) and $\text{Y}(\text{NO}_3)_3$ phase (JCPDS card no. 49-0604) phases. At 700°C , peaks characteristic due to YSrAl_3O_7 phase starts to appear, while the peaks due to strontium nitrate and ytterium nitrate starts to diminish. At this temperature the characteristic peak intensity were weak, but on further heating the sample at 900°C the enhancement of peak intensity is noticed. At 1100°C , all diffraction peaks corresponding to pure crystalline structure YSrAl_3O_7 are observed which matched well with literature data [22]. XRD diffraction peaks of samples calcined at 1100°C are observed to be of high intensity and narrow line width due to better crystallinity and grain growth. The size of the crystallites can be estimated with the help of Scherrer equation, $D = 0.89\lambda/\beta\cos\theta$, where D is the average grain size, λ is X-ray wavelength (0.15418 nm), and θ and β are the diffraction angles and full-width at half-maximum (FWHM, in radian) of an observed peak, respectively [23]. The calculated average particle sizes (D) of $\text{YSrAl}_3\text{O}_7:\text{Tb}^{3+}$ particles are found to be 15, 19 and 22 nm at calcination temperatures 700°C , 900°C and 1100°C respectively. Hence, with increase of temperature the crystal size becomes larger.

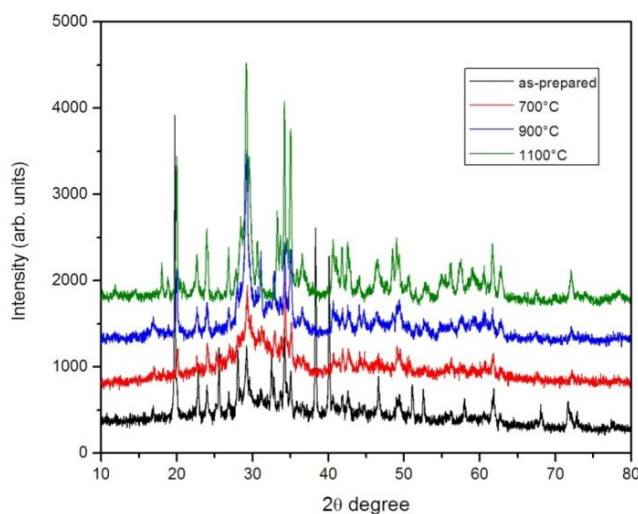


Fig. 1: XRD patterns of $Y_{0.9}Tb_{0.1}SrAl_3O_7$ powders calcined at various temperatures.

3.2. Morphological characteristics

SEM study is carried out to investigate surface morphology and grain size of the synthesized particles. SEM images of $Y_{0.9}Tb_{0.1}SrAl_3O_7$ nanophosphor as synthesized and calcined at 1100°C are displayed in fig. 2. Fig. 2(a) depicts unusual morphology of the as-synthesized products i.e. cracks, voids and porous network due to release of a lot of gaseous by-products during combustion. The SEM micrographs shown in fig. 2(b) reveals that the morphology of the samples calcined at 1100°C , have small and coagulated particles of nearly tetragonal shape, with small size distribution and regular surface. It can be noticed from micrograph that all the particles are densely packed, thus preventing it from aging. TEM image of $Y_{0.9}Tb_{0.1}SrAl_3O_7$ calcined at 1100°C , as shown in fig. 3, present nearly tetragonal and loosely agglomerated particles. Average particle sizes were in the range of 10-20 nm which is in agreement with that estimated by Scherrer's equation.

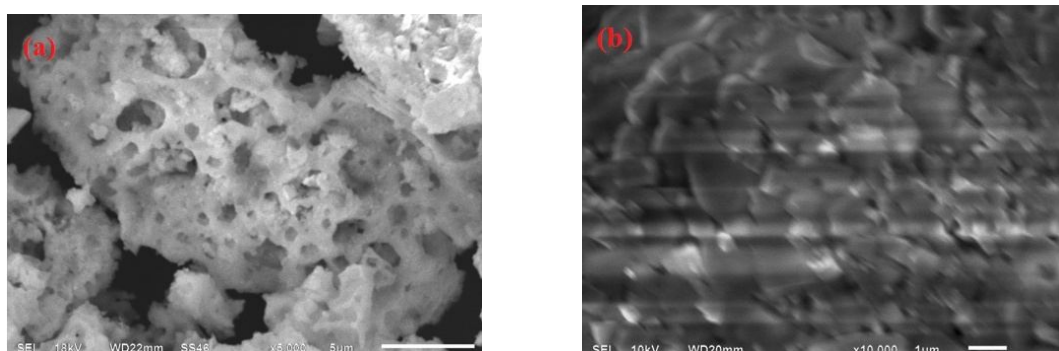


Fig. 2: SEM micrographs of $Y_{0.9}Tb_{0.1}SrAl_3O_7$ (a) as-synthesized; and (b) calcined 1100°C .

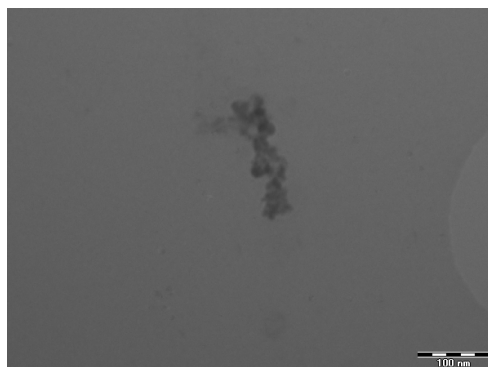


Fig. 3: TEM image of $\text{Y}_{0.9}\text{Tb}_{0.1}\text{SrAl}_3\text{O}_7$ sample calcined at 1100°C .

3.3. Luminescent properties

Fig. 4 shows the excitation spectrum of $\text{Y}_{0.9}\text{Tb}_{0.1}\text{SrAl}_3\text{O}_7$ calcined at 1100°C at an emission wavelength of 544 nm. The excitation spectrum consists of a broad excitation band in the range from 200 to 280 nm with a maximum at about 251 nm and a series of sharp peaks between 300 and 450 nm with very low intensity in comparison to broad band. The high intensity band at 251 nm is assigned to spin-allowed $4f^8-4f^75d^1$ transitions of Tb^{3+} ions in the YSrAl_3O_7 host lattice. The peaks from 300 to 450 nm are assigned to Tb^{3+} intra- $4f$ ($4f^8-4f^8$) transitions from the ground state to higher energy levels. The dominant excitation peaks at 319, 370 and 377 nm can be attributed to ${}^7\text{F}_6-{}^5\text{D}_1$, ${}^7\text{F}_6-{}^5\text{D}_3$ and ${}^7\text{F}_6-{}^5\text{L}_{10}$ transitions of Tb^{3+} , respectively [24,25]. The emission spectrum of $\text{YSrAl}_3\text{O}_7:\text{Tb}^{3+}$ on 251 nm excitation wavelength shows several peaks from 500 to 650 nm as shown in fig. 5. The peaks centered at 544, 589 and 625 nm attributed to ${}^5\text{D}_3-{}^7\text{F}_5$, ${}^5\text{D}_3-{}^7\text{F}_4$ and ${}^5\text{D}_4-{}^7\text{F}_3$ transitions of Tb^{3+} ions, respectively [26,27]. The relative PL intensity of $\text{Y}_{0.9}\text{Tb}_{0.1}\text{SrAl}_3\text{O}_7$ as a function of temperature, at $\lambda_{\text{ex}} = 251$ nm is shown in fig. 5(a). The fig. shows clearly the increasing PL intensity with increase in temperature and maximum is observed at 1100°C temperature.

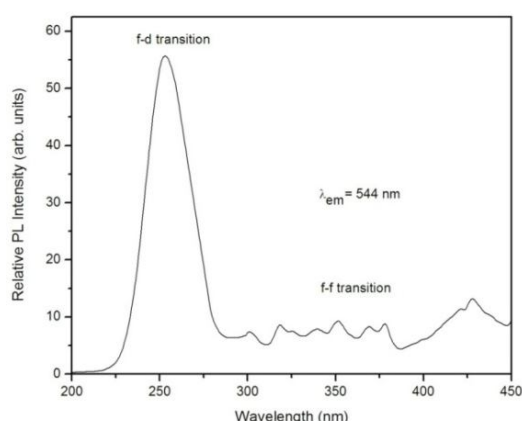


Fig. 4: Excitation spectrum of $\text{Y}_{0.9}\text{Tb}_{0.1}\text{SrAl}_3\text{O}_7$ sample calcined 1100°C , $\lambda_{\text{em}} = 544$ nm.

The luminescence intensities of nanoparticles is dependent on the dopant concentration, hence the variation of emission intensity with Tb^{3+} concentrations in $Y_{1-x}Tb_xSrAl_3O_7$ is depicted in fig. 5(b). It is found that the PL emission intensity of $YSrAl_3O_7:Tb^{3+}$ first increases with the increasing Tb^{3+} concentration reaching a maximum at $x = 0.10$, then it decreases with further increase in Tb^{3+} concentration because of mutual Tb^{3+} - Tb^{3+} interactions.

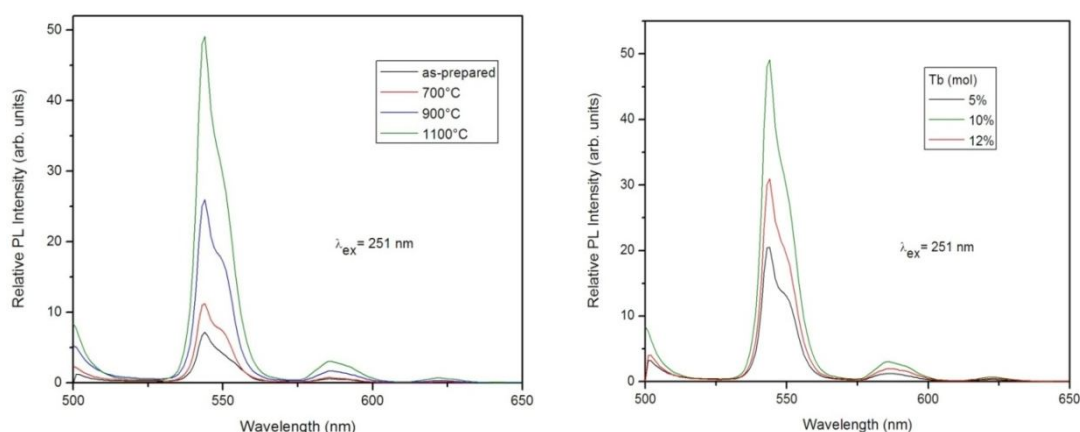


Fig. 5: Emission spectra of $Y_{0.9}Tb_{0.1}SrAl_3O_7$ calcined at different temperatures; (b) Relative PL intensity of $Y_{1-x}SrAl_3O_7:xTb^{3+}$ as a function of temperature, $\lambda_{ex} = 251$ nm.

4. Conclusion

This paper presents yttrium strontium aluminate doped with terbium synthesized by solution combustion method. The PL spectroscopic characterization shows the effect of Tb^{3+} ions on the luminescent properties of host lattice. The emission spectrum of Tb^{3+} doped $YSrAl_3O_7$ shows a dominant peak at 544 nm (green) wavelength on excitation at 251 nm. Furthermore, the phosphors characterized by XRD, SEM and TEM reveal nanosized particles.

References

- [1] W R Romanowski, S Golab, W A Pisarski, G D Dzik, M Berkowski and A Pajaczkowska (1997), Chem. Solids, **58**, pp. 639.
- [2] J G Mahakhode, S J Dhoble, C P Joshi and S V Moharil (2007), J. Alloys Compd., **438**, pp. 293.
- [3] I Pracka, W Giersz, M Swirkowicz, A Pajaczkowska, S Kaczmarek, Z Mierczyk and K Kopczynski (1994), Mater. Sci. Eng. B, **26**, pp. 201.
- [4] X Zhang, J Zhang, L Liang and Q Su (2005), Mater. Res. Bull., **40**, pp. 281.

- [5] S Kubota, M Izumi, H Yamane and M Shimada (1999), *J. Alloys Compd.*, **283**, pp. 95.
- [6] B Liu, D Ding, Z Liu, F Chen and C Xia (2011), *Solid State Ionics*, **191**, pp. 68.
- [7] M A Kale, C P Joshi, S V Moharil, P L Muthal and S M Dhopte (2008), *J. Lumin.*, **128**, pp. 1225.
- [8] W R Romanowski, S Golab, W A Pisarski, G D Dzik, M Berkowski and A Pajaczkowska (1996), *Int. J. Electron.*, **81**, pp. 457.
- [9] Y Huang, L Zhou, L Yang and Z Tang (2011), *Opt. Mater.*, **33**, pp. 777.
- [10] J Zhao, W Zhang, E Xie, Z Liu, J Feng and Z Liu (2011), *Mater. Sci. Eng. B*, **176**, pp. 932.
- [11] P C S Filho and O A Serra (2011), *J. Phys. Chem. C*, **115**, pp. 636.
- [12] H Lai, A Bao, Y Yang, Y Tao, H Yang, Y Zhang and L Han (2008), *J. Phys. Chem. C*, **112**, pp. 282.
- [13] N Kodama, Y Tanii and M Yamaga (2000), *J. Lumin.*, **87-89**, pp. 1076.
- [14] M Malinowski, I Praka, P Myziak, R Piramidowicz and W Wolinski, *J. Lumin.*, **72-74**, pp. 224.
- [15] L Zhou, W C H Choy, J Shi, M Gong, H Liang and T I Yuk (2005), *J. Solid State Chem.*, **178**, pp. 3004.
- [16] A Bao, C Tao and H Yang (2007), *J. Lumin.*, **126**, pp. 859.
- [17] A Bao, H Yang and C Tao (2009), *Curr. Appl. Phys.*, **9**, pp. 1252.
- [18] V Singh, V K Rai, K A Shamery, J Nordmann and M Haase (2011), *J. Lumin.*, **131**, pp. 2679.
- [19] V Singh, S Watanabe, T K Gundu Rao and H Y Kwak (2011), *J. Fluoresc.*, **21**, pp. 313.
- [20] V B Taxak, S P Khatkar, M Kumar and S D Han (2010), *ECS Transactions*, **28**, 3, pp. 161.
- [21] S Ekambaram and K C Patil (1997), *J. Alloys Compd.*, **448**, pp. 7.
- [22] Z G Xia, H Y Du, J Y Sun and X F Wang (2009), *J. Funct. Mater.*, **40**, pp. 1432.
- [23] X Q Zeng, G Y Hong, H P You and X Y Wu (2001), *Chin. J. Lumin.*, **22**, pp. 58.
- [24] Y Yang, A Bao, H Lai, Y Tao and H Yang (2009), *J. Phys. Chem. Solids*, **70**, pp. 1317.
- [25] G Li, Y Lai, W Bao, L Li, M Li, S Gan, T Long and L Zou (2011), *Powder Technol.*, **214**, pp. 211.
- [26] Z J Zhang, J L Yuan, H H Chen, X X Yang, J T Zhao, G B Zhang and C S Shi (2009), *Solid State Sci.*, **11**, pp. 549.
- [27] U Rambabu, D P Amalnerkar, B B Kale and S Buddhudu (2001), *Mater. Chem. Phys.*, **70**, pp. 1.

